

Sparse Interaction Neighborhood Selection for Markov Random Fields via Reversible Jump and Pseudoposteriors

Victor Freguglia
University of Campinas

Nancy Lopes Garcia
University of Campinas

December 15, 2022

Abstract

We consider the problem of estimating the interacting neighborhood of a Markov Random Field model with finite support and homogeneous pairwise interactions based on relative positions of a two-dimensional lattice. Using a Bayesian framework, we propose a Reversible Jump Monte Carlo Markov Chain algorithm that jumps across subsets of a maximal range neighborhood, allowing us to perform model selection based on a marginal pseudoposterior distribution of models. To show the strength of our proposed methodology we perform a simulation study and apply it to a real dataset from a discrete texture image analysis.

1 Introduction

Markov Random Fields on two-dimensional lattices are popular probabilistic models for describing features of digital images in a wide range of applications. Classical problems like image segmentation rely on these models to describe unobserved variables used for pixel classification, see for example [Held et al. \(1997\)](#); [Zhang et al. \(2001\)](#). More general inference-oriented models, such as the ones used in texture modeling problems, describe pixel values directly as a Markov Random Field being first introduced by [Hassner and Sklansky \(1981\)](#); [Cross and Jain \(1983\)](#). For a review of Markov Random Fields in image processing and segmentation see, for example, [Blake et al. \(2011\)](#) and [Kato et al. \(2012\)](#).

A Markov Random Field in a lattice is a collection of random variables whose dependence structure is implicitly defined by a graph. When the edge structure is completely known, one of the main inferential challenges is caused by cycles that prevent expressing the likelihood function as a product of simpler conditional probabilities as in classical Markov Chain models. The impossibility of decomposing the joint probability of a high-dimensional random vector into simpler pieces requires a high-dimensional integral (or sum) in order to

compute the normalizing constant of those probability measures. In general, the normalizing constant directly depends on the parameters of the distribution, thus being an important part of likelihood-based analyses. Whenever this high-dimensional integral cannot be computed in reasonable time, often due to the exponential complexity of a non-independent high-dimensional space, the likelihood function becomes intractable, rendering most of the usual inference and model selection techniques unusable directly.

Inference under intractable likelihoods is a key topic for analyzing high-dimensional data with local dependence. In particular, in a Bayesian context, Monte Carlo Markov Chain (MCMC) methods that generate samples from the posterior distributions under intractability have been developed using different strategies, such as including additional random elements with particular distributions that lead to convenient analytical properties that cancels out the intractable constant (Murray et al., 2012) or generating samples from model configurations that help producing approximations for the intractable likelihood function at each step of the MCMC algorithm (Atchadé et al., 2013) or prior to the Markov Chain iterations (Boland et al., 2018).

Another frequently used approach, introduced in Besag (1975), is to directly substitute the likelihood function term that appears in the posterior distribution for the pseudolikelihood function resulting in an analysis based not on the posterior distribution, but on a function that is referred as the pseudoposterior distribution. While the pseudolikelihood function may differ from the actual likelihood function, inference methods based on pseudolikelihoods have theoretical results available and practical usefulness, including in Bayesian contexts, often including adjustments to the function such as in Bouranis et al. (2017).

Furthermore, the main challenge in dealing with the intractability of likelihood in Markov Random Fields might be the choice of the neighborhood system since most of the common methodologies for model selection are impractical. Although using an approximation of the likelihood function removes most of the probabilistic properties which model selection and hypothesis testing in general rely on, in the context of determining the neighborhood for MRF, pseudolikelihoods have been used by several authors. Among others, we can cite the early work of Ji and Seymour (1996) which proposed its use for Gibbs random fields induced by translation-invariant pair-potentials of finite range, to more recent works, such as Lee and Hastie (2013) which designed algorithms for structure learning in graphical models and, Su and Borsuk (2016), Pensar et al. (2017) and Roy and Dunson (2020) that used pseudoposteriors to find the dependence structure in Markov networks (graphical models). It is worth noticing that Csiszár and Talata (2006) proved that a modification of the Bayesian Information Criteria, replacing the likelihood by the pseudolikelihood, provides strongly consistent estimators of the neighborhood from a single realization of the process observed at increasing regions.

One advantage of studying complex models under a Bayesian framework is that the space of unobserved random quantities may be extended to include not only a vector of real-valued parameters, but also more general objects that can represent models. Including subsets of an arbitrary parameter space and

obtaining distributions from these general objects using MCMC methods tends to be more feasible than constructing efficient optimizations algorithm in such spaces. For example, [Arnesen and Tjelmeland \(2017\)](#) aims to select the dependence structure of an Ising model among a small set of possible candidates with low-dimensional parameter spaces. Additionally, RJMCMC methods ([Green, 1995](#)) provide a framework for constructing a Markov Chain with a generic invariant distribution on general spaces, including varying-dimensional parameter spaces that are highly useful for variable and model selection under a Bayesian philosophy. However, these methods require a careful construction of a proposal kernel in order to be efficient. For instance, [Bouranis et al. \(2018b\)](#) proposes a RJMCMC model selection procedure for the exponential random graph model.

In this work, we propose a pseudoposterior-based procedure for selecting the interaction structure, in a large set of candidate subsets of a maximal structure, on a general class of Markov Random Field models with pairwise interactions based on a set of relative positions as introduced in [Section 2](#), using RJMCMC with a kernel specially constructed for this problem defined in [Section 3](#). To show the strength of our method, in [Section 4](#), we use a simulation study to evaluate the proposed method under different scenarios, and apply the algorithm in a texture synthesis problem with a real dataset in [Section 5](#).

2 Markov Random Fields with Spatially Homogeneous Pairwise Interactions

2.1 Model Description and Definitions

Consider a Markov Random Field (MRF) model on two-dimensional lattices with finite support and non-parametric pairwise interactions as described in [Freguglia et al. \(2020\)](#). The probability function for this model is completely defined by two main elements: *a set of relative positions*, that described the interaction structure of the process, and *a vector of potentials* describing the weights of interactions for each of these relative positions.

Denote by \mathcal{S} a set of sites (also referred as pixels) in a finite n_1 by n_2 two-dimensional lattice

$$\mathcal{S} = \{\mathbf{i} = (i_1, i_2) : 1 \leq i_1 \leq n_1, 1 \leq i_2 \leq n_2\},$$

and $\mathbf{Z} = (Z_{\mathbf{i}})_{\mathbf{i} \in \mathcal{S}}$ a random field indexed by \mathcal{S} , where each $Z_{\mathbf{i}}$ is a random variable assuming values in a finite alphabet denoted \mathcal{Z} . Without loss of generality, we consider $\mathcal{Z} = \{0, 1, \dots, C\}$.

Define a *Relative Position Set (RPS)*, denoted \mathcal{R} , as a finite set of integer vectors $\mathbf{r} \in \mathbb{Z}^2$ without pairs of vectors with opposing directions, i.e.,

$$\mathbf{r} \in \mathcal{R} \implies -\mathbf{r} \notin \mathcal{R},$$

and, given a fixed RPS \mathcal{R} , define a vector of potentials denoted $\boldsymbol{\theta}$, as a vector of real numbers indexed by $\mathcal{Z} \times \mathcal{Z} \times \mathcal{R}$,

$$\boldsymbol{\theta} = (\theta_{a,b,\mathbf{r}})_{a,b \in \mathcal{Z}, \mathbf{r} \in \mathcal{R}}.$$

Given a RPS \mathcal{R} and an associated vector $\boldsymbol{\theta}$, the Markov Random Field with homogeneous pairwise interaction considered in this work is characterized by the probability measure

$$f(\mathbf{z}|\mathcal{R}, \boldsymbol{\theta}) = \frac{1}{\zeta(\boldsymbol{\theta})} \exp \left(\sum_{\mathbf{i} \in \mathcal{S}} \sum_{\mathbf{r} \in \mathcal{R}} \sum_{a=0}^C \sum_{b=0}^C \theta_{a,b,\mathbf{r}} \mathbb{1}_{(z_{\mathbf{i}}=a)} \mathbb{1}_{(z_{\mathbf{i}+\mathbf{r}}=b)} \right), \quad (1)$$

where $\zeta(\boldsymbol{\theta}) = \sum_{\mathbf{z}' \in \mathcal{Z}^{|\mathcal{S}|}} \exp \left(\sum_{\mathbf{i} \in \mathcal{S}} \sum_{\mathbf{r} \in \mathcal{R}} \sum_{a=0}^C \sum_{b=0}^C \theta_{a,b,\mathbf{r}} \mathbb{1}_{(z'_{\mathbf{i}}=a)} \mathbb{1}_{(z'_{\mathbf{i}+\mathbf{r}}=b)} \right)$ is a normalizing constant, with the convention that the term $\mathbb{1}_{(z'_{\mathbf{i}}=a)}$ is treated as 0 if $\mathbf{i}' \notin \mathcal{S}$ for every $a \in \mathcal{Z}$. This ensures that the sum terms are consistently defined across every pair of positions in \mathcal{S} that are within a relative position in \mathcal{R} . [Figure 1](#) presents an illustration of how the terms $\sum_{\mathbf{r} \in \mathcal{R}} \theta_{z_{\mathbf{i}}, z_{\mathbf{i}+\mathbf{r}}, \mathbf{r}}$ are computed for some positions \mathbf{i} of an example field \mathbf{z} .

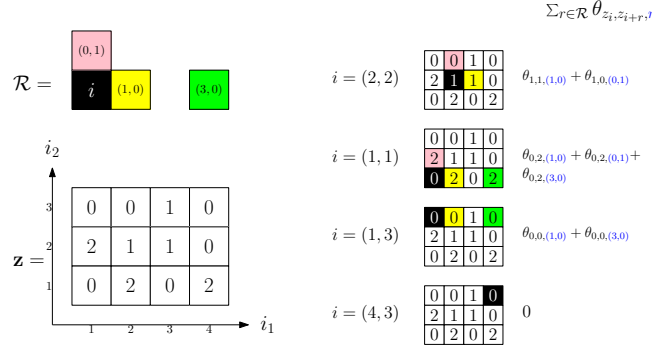


Figure 1: An example field \mathbf{z} with dimensions $n_1 = 4$, $n_2 = 3$ and the computed sums $\sum_{\mathbf{r} \in \mathcal{R}} \theta_{z_{\mathbf{i}}, z_{\mathbf{i}+\mathbf{r}}, \mathbf{r}}$ for some positions \mathbf{i} considering a RPS $\mathcal{R} = \{(1,0), (0,1), (3,0)\}$.

In (1), adding a constant value to the potentials $\theta_{a,b,\mathbf{r}}$ associated with every pair $a, b \in \mathcal{Z}$ and a fixed relative position \mathbf{r} , causes the value of $f(\mathbf{z}, \mathcal{R}, \boldsymbol{\theta})$ to be unchanged, as the resulting scale change is also reflected in the normalizing constant $\zeta(\boldsymbol{\theta})$. In other words, two different vector of potentials $\boldsymbol{\theta}$ may have the same likelihood, therefore, leading to a non-identifiability problem. In order to obtain identifiability, additional constraints are required and, following [Freguglia et al. \(2020\)](#), we adopt the zero-valued reference pair $((a, b) = (0, 0))$ constraint

$$\theta_{0,0,\mathbf{r}} = 0 \text{ for all } \mathbf{r} \in \mathcal{R}.$$

Note that, while we still use the term $\theta_{0,0,\mathbf{r}}$ in some equations, for simplicity of notation, we will not consider these indexes in the vector $\boldsymbol{\theta}$. Additionally, the vector $\boldsymbol{\theta}$ can be expressed in terms of subvectors $\boldsymbol{\theta} = (\boldsymbol{\theta}_{\mathbf{r}})_{\mathbf{r} \in \mathcal{R}}$, where each subvector $\boldsymbol{\theta}_{\mathbf{r}} = (\theta_{a,b,\mathbf{r}})_{(a,b) \in \mathcal{Z}^2, (a,b) \neq (0,0)}$ corresponds to non-null potentials associated with a single relative position \mathbf{r} and we denote by d the dimension of $\boldsymbol{\theta}_{\mathbf{r}}$, which is given by $d = (|\mathcal{Z}|)^2 - 1$.

2.2 Conditional Probabilities and Pseudolikelihood

While the MRF model introduced is well-defined, inference for such model gets problematic on non-trivial cases due to the intractability of the normalizing constant, $\zeta(\boldsymbol{\theta})$, as it requires computing a sum of an exponential number of terms, $(|\mathcal{Z}|)^{n_1 n_2}$, which quickly becomes infeasible. For example, even for $n_1 = n_2 = 100$, which is not even considered large for common applications, computing the normalizing constant is impractical.

One of the most important features of MRF models is local dependence that makes probability functions decomposable into a product of functions that depend on \mathbf{z} only through subsets of it, like pairs $(z_{\mathbf{i}}, z_{\mathbf{i}+\mathbf{r}})$, in the case of (1). This decomposition allows expressing the conditional probability of specific $z_{\mathbf{i}}$ given every other element $\mathbf{z}_{-\mathbf{i}} = \{z_{\mathbf{i}'} : \mathbf{i}' \in \mathcal{S}, \mathbf{i}' \neq \mathbf{i}\}$ as

$$f(z_{\mathbf{i}}|\mathbf{z}_{-\mathbf{i}}, \mathcal{R}, \boldsymbol{\theta}) = f(z_{\mathbf{i}}|\mathbf{z}_{\mathcal{N}_{\mathbf{i}}}, \mathcal{R}, \boldsymbol{\theta}) = \frac{\exp\left(\sum_{\mathbf{r} \in \mathcal{R}} \theta_{z_{\mathbf{i}}, z_{\mathbf{i}+\mathbf{r}}, \mathbf{r}} + \theta_{z_{\mathbf{i}-\mathbf{r}}, z_{\mathbf{i}}, \mathbf{r}}\right)}{\sum_{a \in \mathcal{Z}} \exp\left(\sum_{\mathbf{r} \in \mathcal{R}} \theta_{a, z_{\mathbf{i}+\mathbf{r}}, \mathbf{r}} + \theta_{z_{\mathbf{i}-\mathbf{r}}, a, \mathbf{r}}\right)}, \quad (2)$$

where $\mathcal{N}_{\mathbf{i}} \subset \mathcal{S}$ denotes the set of neighbors of \mathbf{i} based on the RPS \mathcal{R} , i.e., $\mathcal{N}_{\mathbf{i}} = \{\mathbf{i}' : \mathbf{i}' \in \mathcal{S} \text{ and } \mathbf{i}' = \mathbf{i} \pm \mathbf{r}, \mathbf{r} \in \mathcal{R}\}$.

The computationally simple expressions for conditional probabilities on (2) allows the use of alternative functions based on conditional probabilities instead of the joint probability. For problems with high-dimensional dependent data, when conditional probabilities are available and simple, a function widely used as a proxy for the likelihood function is the **pseudolikelihood function** from Besag (1975), defined as the product of conditional probabilities evaluated at the observed values, $z_{\mathbf{i}}$,

$$\tilde{f}(\mathbf{z}|\mathcal{R}, \boldsymbol{\theta}) = \prod_{\mathbf{i} \in \mathcal{S}} f(z_{\mathbf{i}}|\mathbf{z}_{\mathcal{N}_{\mathbf{i}}}, \mathcal{R}, \boldsymbol{\theta}). \quad (3)$$

Note that while the normalizing constant $\zeta(\boldsymbol{\theta})$ from (1) requires a sum over $(|\mathcal{Z}|)^{|\mathcal{S}|}$ random field configurations, (3) involves $|\mathcal{S}|$ normalizing constants that are sums over $|\mathcal{Z}|$ terms. Thus, the computational cost for evaluating the pseudolikelihood is $\mathcal{O}(|\mathcal{Z}| \times |\mathcal{S}|)$, while the exact likelihood function has a cost of order $\mathcal{O}(|\mathcal{Z}|^{|\mathcal{S}|})$.

3 A Bayesian Framework for Sparse Interaction Structure Selection

In a Bayesian context, unobservable quantities, for example the parameters of a model, are considered unobserved random variables with specific prior distributions defined beforehand. Many Bayesian model selection methodologies extend this concept by assuming that not only a set of real-valued parameters (the vector of free potentials $\boldsymbol{\theta}$ within the scope of this work) is a vector of

random variables, but also the model itself (interpreted as the RPS \mathcal{R}) is an unobserved random object with its given prior distribution.

Considering a collection of proper RPSs denoted \mathcal{M} , we can define a Bayesian system hierarchically by

$$\begin{aligned}\mathcal{R} &\sim q(\mathcal{R}), & \mathcal{R} &\in \mathcal{M}, \\ \boldsymbol{\theta}|\mathcal{R} &\sim \phi(\boldsymbol{\theta}|\mathcal{R}), & \boldsymbol{\theta} &\in \mathbb{R}^{d|\mathcal{R}|}, \\ \mathbf{z}|\mathcal{R}, \boldsymbol{\theta} &\sim f(\mathbf{z}|\mathcal{R}, \boldsymbol{\theta}), & \mathbf{z} &\in \mathcal{Z}^{|\mathcal{S}|},\end{aligned}$$

where $q(\mathcal{R})$ is the prior distribution of the RPS, $\phi(\boldsymbol{\theta}|\mathcal{R})$ is the prior distribution of the parameter vector $\boldsymbol{\theta}$ given a particular RPS \mathcal{R} and $f(\mathbf{z}|\mathcal{R}, \boldsymbol{\theta})$ is the probability function of a MRF as in (1).

Given that the support of \mathcal{R} represents the sets of interacting positions, a natural choice for the collection of candidate models \mathcal{M} is the power set of a **maximal RPS**, denoted \mathcal{R}_{\max} ,

$$\mathcal{M} = \{\mathcal{R}' : \mathcal{R}' \subset \mathcal{R}_{\max}\},$$

which contains $2^{|\mathcal{R}_{\max}|}$ possible neighborhoods. For simplicity of notation, we shall use $\boldsymbol{\theta}$ to denote a vector of varying dimension, which indexing is always associated with an interaction structure \mathcal{R} . The dimension, $d|\mathcal{R}|$, and indexing of $\boldsymbol{\theta} = (\boldsymbol{\theta}_{\mathbf{r}})_{\mathbf{r} \in \mathcal{R}}$ are always implicitly specified as the vector is consistently matched with an interaction structure \mathcal{R} in every expression. Note that, within this scope, we are referring as a model to the RPS that defines the interaction structure of a MRF. This problem can also be interpreted as a variable selection problem as any vector of interaction coefficients associated with a RPS \mathcal{R} , with restrictions that $\boldsymbol{\theta}_{a,b,\mathbf{r}} = 0$ for all a, b for specific \mathbf{r} , can also be expressed (in terms of identical likelihood values) to a model excluding \mathbf{r} from \mathcal{R} .

In a model selection context, our main interest is to find the marginal posterior distribution of a model $\pi(\mathcal{R}|\mathbf{z})$, which can be obtained by integrating the (complete) posterior distribution,

$$\pi(\mathcal{R}, \boldsymbol{\theta}|\mathbf{z}) = \frac{q(\mathcal{R})\phi(\boldsymbol{\theta}|\mathcal{R})f(\mathbf{z}|\mathcal{R}, \boldsymbol{\theta})}{\sum_{\mathcal{R}' \in \mathcal{M}} q(\mathcal{R}') \int_{\mathbb{R}^{d|\mathcal{R}'|}} \phi(\boldsymbol{\theta}'|\mathcal{R}')f(\mathbf{z}|\mathcal{R}', \boldsymbol{\theta}')d\boldsymbol{\theta}'}, \quad (4)$$

with respect to $\boldsymbol{\theta}$.

Two main computational challenges arise from (4) making most direct analyses prohibitively complex: (I) $f(\mathbf{z}|\mathcal{R}, \boldsymbol{\theta})$ cannot be evaluated directly due to the intractable normalizing constant and (II) the denominator involves $2^{|\mathcal{M}|}$ integrations, possibly including many high-dimensional functions that have intractable normalizing constants. Because of these two sources of intractability, this type of posterior distribution is often referred in the literature as a doubly-intractable distribution (Murray et al., 2012; Caimo and Mira, 2015).

Monte Carlo Markov Chain methods are used to generate an ergodic Markov Chain which invariant distribution is equal to a specific target distribution which, in most cases, is a posterior distribution with intractable normalizing

constant like (4). Consider an ergodic Markov chain in the space that is a product of \mathcal{M} by the space of real vectors with varying dimension directly associated with the element of \mathcal{M} , i.e., $(\mathcal{R}^{(1)}, \boldsymbol{\theta}^{(1)}), (\mathcal{R}^{(2)}, \boldsymbol{\theta}^{(2)}), \dots$, such that $\boldsymbol{\theta}^{(t)} \in \mathbb{R}^{d|\mathcal{R}^{(t)}|}$, and invariant measure $\pi(\cdot, \cdot | \mathbf{z})$. Then, due to the ergodic theorem, for any bounded function g of the form

$$g : \mathcal{M} \times \bigcup_{k=0}^{|\mathcal{R}_{\max}|} \mathbb{R}^{dk} \rightarrow \mathbb{R},$$

we have

$$\sum_{t=1}^n g(\mathcal{R}^{(t)}, \boldsymbol{\theta}^{(t)}) \rightarrow \mathbb{E}_{\pi}(g(\mathcal{R}, \boldsymbol{\theta}) | \mathbf{z}), \quad \text{a.s.} \quad (5)$$

where $\mathbb{E}_{\pi}(g(\mathcal{R}, \boldsymbol{\theta}) | \mathbf{z})$ is the conditional expected value of the random variable $g(\mathcal{R}, \boldsymbol{\theta})$ given the observed \mathbf{z} , under the (target) distribution $\pi(\mathcal{R}, \boldsymbol{\theta} | \mathbf{z})$. Some particular choices of g lead to interpretable quantities, that are useful for evaluating the plausibility of interaction neighborhoods \mathcal{R} based on their posterior distribution, such as $g(\mathcal{R}, \boldsymbol{\theta}) = \mathbb{1}(\mathcal{R} = \mathcal{R}^*)$, which results in (5) being the posterior probability of a particular neighborhood \mathcal{R}^* or $g(\mathcal{R}, \boldsymbol{\theta}) = \mathbb{1}(\mathbf{r} \in \mathcal{R})$, which corresponds to the marginal posterior probability that a particular relative position \mathbf{r} belongs to the RPS.

Given the estimated marginal posterior probabilities for each position in \mathcal{R}_{\max} , obtained from a Metropolis-Hastings sample of size T , and a threshold value c_{th} , a sparse estimator of the RPS, denoted $\hat{\mathcal{R}}_{\text{sp}}(c_{\text{th}})$, can be obtained by selecting the set of all positions with (estimated) posterior probability exceeding c_{th} ,

$$\hat{\mathcal{R}}_{\text{sp}}(c_{\text{th}}) = \{\mathbf{r} \in \mathcal{R}_{\max} : \frac{1}{T} \sum_{t=1}^T \mathbb{1}(\mathbf{r} \in \mathcal{R}^{(t)}) > c_{\text{th}}\}. \quad (6)$$

3.1 Pseudoposterior-based inference

In order to overcome the computational infeasibility due to the intractable normalizing constant of the likelihood function f defined in (1), many methods for inference on MRFs have been proposed. One of the commonly used approaches is to replace the likelihood function, f , for the pseudolikelihood, \tilde{f} , defined in (3), which can be evaluated directly.

When applied to the Bayesian system defined in the previous section, this replacement of the likelihood function leads to an alternative function referred as pseudoposterior distribution, that is proportional to the product of prior distributions and the pseudolikelihood, and it is formally defined as (*cf.* with (4))

$$\tilde{\pi}(\mathcal{R}, \boldsymbol{\theta} | \mathbf{z}) = \frac{q(\mathcal{R}) \phi(\boldsymbol{\theta} | \mathcal{R}) \tilde{f}(\mathbf{z} | \mathcal{R}, \boldsymbol{\theta})}{\sum_{\mathcal{R}' \in \mathcal{M}} q(\mathcal{R}') \int_{\mathbb{R}^{d|\mathcal{R}'|}} \phi(\boldsymbol{\theta}' | \mathcal{R}') \tilde{f}(\mathbf{z} | \mathcal{R}', \boldsymbol{\theta}') d\boldsymbol{\theta}'}. \quad (7)$$

It is valuable to note that, while the pseudolikelihood is a plausible proxy for the likelihood function in terms of optimization-related mathematical properties, these functions may have different overall shapes depending on how much dependence exists on the dataset considered, and composing functions using the pseudolikelihood instead of the likelihood alters how these functions are interpreted. As a consequence, Bayesian inference based on pseudoposterior produces useful quantities, but the information obtained cannot be interpreted in the conventional way. For example, integrating the pseudoposterior distribution over θ does not result exactly in the posterior distribution of the RPSs \mathcal{R} , but a different measure conceivably useful for evaluating the plausibility of the RPSs.

3.2 A Reversible Jump Proposal Kernel for Sparse Neighborhood Detection

Constructing a proposal kernel for the Metropolis-Hastings algorithm that can efficiently move through both the model space \mathcal{M} and the space of interaction coefficients within a model is not a simple task. [Green \(1995\)](#) proposes the Reversible Jump Monte Carlo Markov Chain (RJMCMC) as a framework for Bayesian analysis of models and varying dimension parameters simultaneously. In general, the strategy consists of composing a proposal kernel which is a mixture of simpler kernels, some proposing within-model moves that only changes parameter values and others proposing reversible jumps between models that have good analytical or computational properties.

In this work, we construct a customized proposal kernel for the model inspired on properties and examples from [Brooks et al. \(2003\)](#) with additional features that are specifically designed for neighborhood selection for MRFs. This proposal kernel consists of a mixture of 4 types of moves seeking to come up with states that might have higher pseudoposterior density than the current state with some probability.

Within-model random walk. The first and simplest move consists of adding a random walk term to the current value of the parameter vector. Given a current pair (\mathcal{R}, θ) , we keep the same neighborhood, $\mathcal{R}' = \mathcal{R}$, and propose a new vector of interaction coefficients $\theta' \in \mathcal{Z}^{d|\mathcal{R}|}$ by adding a Gaussian noise term with matching dimension, each coordinate being independent and identically distributed with mean 0 and variance σ_w^2 , where σ_w^2 is a tuning parameter of the algorithm.

The transition kernel density for this move is given by

$$\kappa_w(\theta', \mathcal{R}' | \theta, \mathcal{R}) = \frac{1}{(2\pi\sigma_w^2)^{d|\mathcal{R}|/2}} \exp\left(-\frac{1}{2\sigma_w^2} \sum_{\mathbf{r} \in \mathcal{R}} (\theta_{\mathbf{r}} - \theta'_{\mathbf{r}})^\top (\theta_{\mathbf{r}} - \theta'_{\mathbf{r}})\right) \mathbb{1}(\mathcal{R}' = \mathcal{R}),$$

making this proposal density not only reversible, but also symmetrical, i.e., $\kappa_w(\theta', \mathcal{R}' | \theta, \mathcal{R}) = \kappa_w(\theta, \mathcal{R} | \theta', \mathcal{R}')$. Since proposed states keep the same inter-

action structure, we also have $q(\mathcal{R}) = q(\mathcal{R}')$, so the terms corresponding to the neighborhood interaction structure are also cancelled in the acceptance ratio.

While this move does not contribute to jumping between RPSs, its goal is to add small incremental changes in the parameter coordinates so that the chain gradually moves towards higher pseudoposterior density regions within a model. Typically, small values of σ_w^2 are preferred so that the coefficients within a RPS are slowly drifting towards the maximum pseudoposterior vector for that RPS.

Birth and Death. We propose a jump move from a state $(\mathcal{R}, \boldsymbol{\theta})$ to a state $(\mathcal{R}', \boldsymbol{\theta}')$, $\mathcal{R}' \neq \mathcal{R}$, by either including a position from \mathcal{R}_{\max} that is not already in \mathcal{R} , or by removing one of the positions in \mathcal{R} . We refer to these moves as Birth and Death of a relative position, respectively.

We define the RPS comparison operator $\overset{\mathbf{r}}{\prec}$ as

$$\mathcal{R} \overset{\mathbf{r}}{\prec} \mathcal{R}' \iff \mathcal{R} \subset \mathcal{R}', \mathbf{r} \notin \mathcal{R} \text{ and } \mathcal{R} \cup \{\mathbf{r}\} = \mathcal{R}',$$

which means that \mathcal{R}' can be obtained by adding the position \mathbf{r} to \mathcal{R} . Given a current RPS \mathcal{R} , we randomly select a position \mathbf{r}^* from \mathcal{R}_{\max} with uniform probabilities $\frac{1}{|\mathcal{R}_{\max}|}$. Then either a birth or death move is proposed depending on the selected \mathbf{r}^* .

- If $\mathbf{r}^* \in \mathcal{R}$, the proposed RPS \mathcal{R}' is such that $\mathcal{R}' \overset{\mathbf{r}^*}{\prec} \mathcal{R}$, i.e., \mathbf{r}^* is removed from \mathcal{R} . For the associated interaction coefficients $\boldsymbol{\theta}'$ to be proposed with \mathcal{R}' , all the values are kept the same $\boldsymbol{\theta}'_{\mathbf{r}} = \boldsymbol{\theta}_{\mathbf{r}}$ for $\mathbf{r} \in \mathcal{R}'$.
- If $\mathbf{r}^* \notin \mathcal{R}$, \mathcal{R}' is proposed by including \mathbf{r}^* , i.e., $\mathcal{R} \overset{\mathbf{r}^*}{\prec} \mathcal{R}'$. For the proposed parameter $\boldsymbol{\theta}'$, we keep the values of the previous $\boldsymbol{\theta}'_{\mathbf{r}} = \boldsymbol{\theta}_{\mathbf{r}}$ for the previously included positions $\mathbf{r} \in \mathcal{R}$ and sample a new vector of i.i.d. Gaussian variables with mean 0 and variance σ_{bd}^2 to assign to $\boldsymbol{\theta}'_{\mathbf{r}^*}$.

Note that, by this definition, transitions between states with two different RPSs \mathcal{R} and \mathcal{R}' are allowed if, and only if, $|\mathcal{R} \nabla \mathcal{R}'| = 1$, where ∇ denotes the symmetrical difference operator for two sets. Therefore, the proposal kernel density for a birth/death jump move is given by

$$\kappa_{\text{bd}}(\boldsymbol{\theta}', \mathcal{R}' | \boldsymbol{\theta}, \mathcal{R}) = \begin{cases} \frac{1}{|\mathcal{R}_{\max}|} \frac{\exp\left(-\frac{1}{2\sigma_{\text{bd}}^2} \boldsymbol{\theta}'_{\mathbf{r}^*} \boldsymbol{\theta}'_{\mathbf{r}^*}^\top\right)}{(2\pi\sigma_{\text{bd}}^2)^{d/2}} \prod_{\mathbf{r} \in \mathcal{R}} \mathbb{1}(\boldsymbol{\theta}'_{\mathbf{r}} = \boldsymbol{\theta}_{\mathbf{r}}) & , \text{ if } \mathcal{R} \overset{\mathbf{r}^*}{\prec} \mathcal{R}', \\ \frac{1}{|\mathcal{R}_{\max}|} \prod_{\mathbf{r} \in \mathcal{R}'} \mathbb{1}(\boldsymbol{\theta}'_{\mathbf{r}} = \boldsymbol{\theta}_{\mathbf{r}}) & , \text{ if } \mathcal{R}' \overset{\mathbf{r}^*}{\prec} \mathcal{R}, \\ 0 & , \text{ if } |\mathcal{R} \nabla \mathcal{R}'| \neq 1. \end{cases}$$

Figure 2 illustrates how new states $(\mathcal{R}', \boldsymbol{\theta}')$ are proposed from a current $(\mathcal{R}, \boldsymbol{\theta})$ when a randomly selected position \mathbf{r}^* is included or not included in \mathcal{R} . It is straightforward to conclude from the example that this type of jump can be reversed by selecting the same position \mathbf{r}^* and, the case of adding a new position, sampling the appropriate $\boldsymbol{\theta}'_{\mathbf{r}^*}$, therefore, $\kappa_{\text{bd}}(\boldsymbol{\theta}', \mathcal{R}' | \boldsymbol{\theta}, \mathcal{R}) > 0$ if, and only if, $\kappa_{\text{bd}}(\boldsymbol{\theta}, \mathcal{R} | \boldsymbol{\theta}', \mathcal{R}') > 0$.

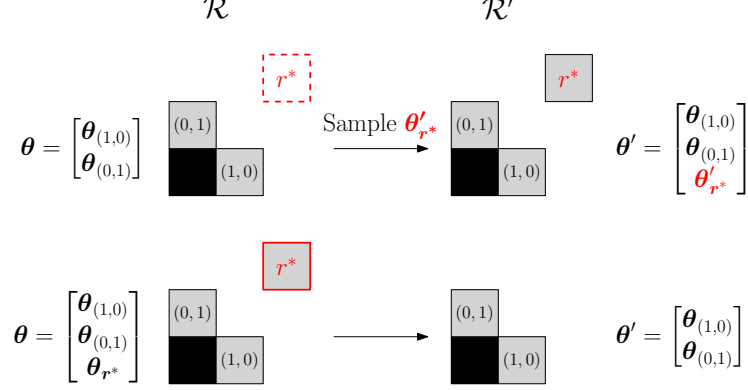


Figure 2: Illustration of a Birth/Death Jump proposal when sampling $\mathbf{r}^* \notin \mathcal{R}$ (top) and $\mathbf{r}^* \in \mathcal{R}$ (bottom).

Position swap. As second type of move constructed for proposing jumps between states with different RPS is to swap one of positions in the current RPS, $\mathbf{r}_{\text{in}} \in \mathcal{R}$, for another one $\mathbf{r}_{\text{out}} \in \mathcal{R}_{\text{max}} \setminus \mathcal{R}$, while keeping all of the interaction coefficients the same, including the subvector associated with the swapped position, $\theta'_{\mathbf{r}_{\text{out}}} = \theta_{\mathbf{r}_{\text{in}}}$. Figure 3 illustrates an example of the position swap move.

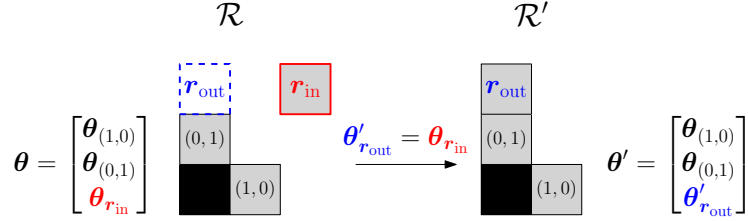


Figure 3: Illustration of a Position swap move proposal.

The positions \mathbf{r}_{in} and \mathbf{r}_{out} , for the swap move, are chosen independently and uniformly distributed on \mathcal{R} and $\mathcal{R}_{\text{max}} \setminus \mathcal{R}$, respectively. Therefore, for any states (θ, \mathcal{R}) and (θ', \mathcal{R}') such that $|\mathcal{R}| = |\mathcal{R}'|$ and $|\mathcal{R} \nabla \mathcal{R}'| = 2$, differing only in the presence of relative positions $\mathbf{r}_{\text{in}} \in \mathcal{R}$ and $\mathbf{r}_{\text{out}} \in \mathcal{R}'$, the proposal density for the swap move is given by

$$\kappa_{\text{sw}}(\theta', \mathcal{R}' | \theta, \mathcal{R}) = \frac{1}{|\mathcal{R}| |\mathcal{R}_{\text{max}} \setminus \mathcal{R}|} \prod_{\mathbf{r} \in \mathcal{R} \cap \mathcal{R}'} \mathbb{1}(\theta_{\mathbf{r}} = \theta'_{\mathbf{r}}) \mathbb{1}(\theta_{\mathbf{r}_{\text{in}}} = \theta'_{\mathbf{r}_{\text{out}}}). \quad (8)$$

Note that (8) is a symmetrical kernel since the inverse operation is proposed by selecting the same pair of positions \mathbf{r}_{in} and \mathbf{r}_{out} reversed, the RPS prior probability only depends on the size of the current RPS, $|\mathcal{R}|$, and we have

the condition that $|\mathcal{R}| = |\mathcal{R}'|$ for every pair of states with positive proposal probability.

The rationale behind this move is that, due to the spatial dependence intrinsic to lattice-based indexing of the MRF model considered, the counts of pairwise configurations in some relative positions may present high correlation, especially when those relative positions are close (e.g. \mathbf{r} and $\mathbf{r} + (1, 0)$) or a multiple one from another (e.g. \mathbf{r} and $2\mathbf{r}$).

Note that while the same jumps proposed by swap moves could be achieved by a series of birth and death moves, one of those steps would be to exclude a relative position, \mathbf{r}_{in} , with associated interaction coefficient, $\theta_{\mathbf{r}_{\text{in}}}$, possibly far from the zero vector, what would cause the acceptance of such move to be highly unlikely. Thus, swap moves is a proposal step that avoids the algorithm getting stuck at a local (with respect to RPSs) maxima, by adding direct connections to states with different RPSs that may have similar pseudoposterior values, taking into account very specific characteristics of the model.

Split and Merge. While the position swap move is proposed in order to allow a relative position included in a state to be substituted by another one that is not included but has a similar pseudoposterior value, another type of local maxima may exist when two or more relative positions with highly correlated sufficient statistics are included in a model simultaneously.

The correlation between vectors of sufficient statistics may cause interaction weights for some relative positions $\theta_{\mathbf{r}}$ to become very unstable, due to the possibility of compensating shifts in one direction for one of the vectors with equivalent shifts in the opposite direction.

We define the Split and Merge moves as a pair of reversible operations that not only allow jumps between different RPSs but also control the values of $\theta_{\mathbf{r}}$ involved. This transition has the goal of redistributing the interactions coefficients, allowing smaller or larger RPSs with similar likelihood to be proposed with some probability. The Merge move permits excessive relative positions to be removed from the current state and possibly generates a proposed state that distributes the interaction weights $\theta_{\mathbf{r}}$ of the position to be removed, by adding it to the remaining positions, hopefully keeping the pseudolikelihood values on similar levels. The key premise on this pair of moves is that, for a pair of states (\mathcal{R}, θ) and (\mathcal{R}', θ') , we have

$$\sum_{\mathbf{r} \in \mathcal{R}} \theta_{\mathbf{r}} = \sum_{\mathbf{r} \in \mathcal{R}'} \theta'_{\mathbf{r}}.$$

Given a current state (\mathcal{R}, θ) , the process of proposing a state (\mathcal{R}', θ') with a **Split** move is composed by the steps of

1. Sample a new position \mathbf{r}^* to be included from $\mathcal{R}_{\text{max}} \setminus \mathcal{R}$ with uniform probability.
2. Generate a new interaction coefficient vector $\theta'_{\mathbf{r}^*}$ from a d -dimensional independent Gaussian distribution with variances σ_s^2 , where the split variance, σ_s^2 , is a tuning parameter of the algorithm.

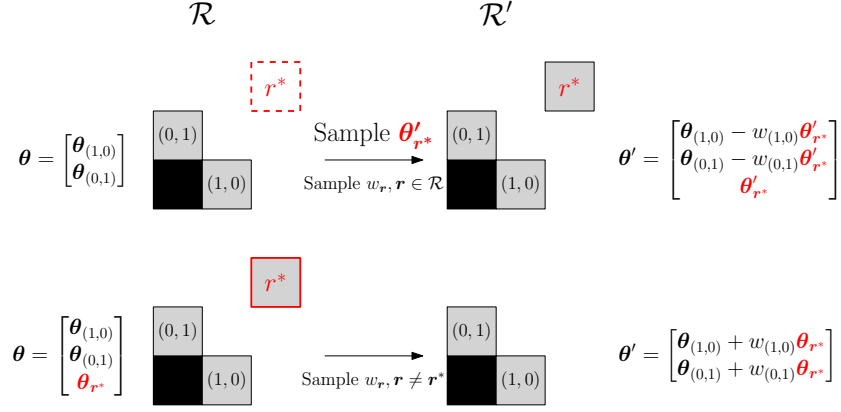


Figure 4: Illustration of Split (top) and Merge (bottom) moves.

3. Generate a vector of weights $\mathbf{w} = (w_{\mathbf{r}})_{\mathbf{r} \in \mathcal{R}}$ from a symmetric Dirichlet distribution with all parameters equal to ν , where ν is another tuning parameter of the algorithm.
4. Propose $\mathcal{R}' = \mathcal{R} \cup \mathbf{r}^*$ and θ' such that $\theta'_{\mathbf{r}^*}$ is the generated vector and $\theta'_{\mathbf{r}} = \theta_{\mathbf{r}} - w_{\mathbf{r}} \theta'_{\mathbf{r}^*}$ for every other relative position $\mathbf{r} \in \mathcal{R}$.

The proposal density for a Split move, κ_s , is given by

$$\kappa_s(\theta', \mathcal{R}' | \theta, \mathcal{R}) = \frac{\prod_{\mathbf{r}^* \in \mathcal{R}_{\max} \setminus \mathcal{R}} \mathbb{1}(\mathcal{R} \prec^{\mathbf{r}^*} \mathcal{R}') \exp\left(\frac{-(\theta'_{\mathbf{r}^*}^\top \theta'_{\mathbf{r}^*})}{2\sigma_s^2}\right)}{|\mathcal{R}_{\max} \setminus \mathcal{R}| (2\pi\sigma_s^2)^{d/2}} \frac{\Gamma(|\mathcal{R}|\nu)}{\prod_{\mathbf{r} \in \mathcal{R}} (\Gamma(\nu))} \prod_{\mathbf{r} \in \mathcal{R}} \left[\left(\frac{\theta_{0,1,\mathbf{r}} - \theta'_{0,1,\mathbf{r}}}{\theta'_{0,1,\mathbf{r}^*}} \right)^{\nu-1} \times \frac{\mathbb{1}\left(0 < \frac{\theta_{0,1,\mathbf{r}} - \theta'_{0,1,\mathbf{r}}}{\theta'_{0,1,\mathbf{r}^*}} < 1\right)}{\theta'_{0,1,\mathbf{r}^*}} \right] \mathbb{1}\left(\sum_{\mathbf{r} \in \mathcal{R}} (\theta_{\mathbf{r}} - \theta'_{\mathbf{r}}) = \theta'_{\mathbf{r}^*}\right) \prod_{a,b \in \mathcal{Z}^2} \mathbb{1}\left(\frac{\theta_{a,b,\mathbf{r}} - \theta'_{a,b,\mathbf{r}}}{\theta'_{a,b,\mathbf{r}^*}} = \frac{\theta_{0,1,\mathbf{r}} - \theta'_{0,1,\mathbf{r}}}{\theta'_{0,1,\mathbf{r}^*}}\right).$$

The **Merge** proposal move is the reverse of the Split move and can be described by the following sequence of steps

1. Sample a state \mathbf{r}^* from \mathcal{R} , which interaction coefficient vector will be merged into the others, with uniform probabilities.
2. Generate a vector of weights $\mathbf{w} = (w_{\mathbf{r}})_{\mathbf{r} \in (\mathcal{R} \setminus \mathbf{r}^*)}$ with Dirichlet distribution with all parameters equal to ν .
3. Propose $\mathcal{R}' = \mathcal{R} \setminus \mathbf{r}^*$ and θ' such that $\theta'_{\mathbf{r}} = \theta_{\mathbf{r}} + w_{\mathbf{r}} \theta_{\mathbf{r}^*}$ for each $\mathbf{r} \in \mathcal{R}'$.

The proposal density for a Merge move is

$$\kappa_m(\boldsymbol{\theta}', \mathcal{R}' | \boldsymbol{\theta}, \mathcal{R}) = \frac{\prod_{\mathbf{r}^* \in \mathcal{R}} \mathbb{1}(\mathcal{R}' \prec^* \mathcal{R})}{|\mathcal{R}|} \frac{\Gamma(|\mathcal{R}'| \nu)}{\prod_{\mathbf{r} \in \mathcal{R}'} (\Gamma(\nu))} \prod_{\mathbf{r} \in \mathcal{R}'} \left[\left(\frac{\theta'_{0,1,\mathbf{r}} - \theta_{0,1,\mathbf{r}}}{\theta_{0,1,\mathbf{r}^*}} \right)^{\nu-1} \times \frac{\mathbb{1}\left(0 < \frac{\theta'_{0,1,\mathbf{r}} - \theta_{0,1,\mathbf{r}}}{\theta_{0,1,\mathbf{r}^*}} < 1\right)}{\theta_{0,1,\mathbf{r}^*}} \right] \mathbb{1}\left(\sum_{\mathbf{r} \in \mathcal{R}'} \boldsymbol{\theta}'_{\mathbf{r}} - \boldsymbol{\theta}_{\mathbf{r}} = \boldsymbol{\theta}_{\mathbf{r}^*}\right) \prod_{a,b \in \mathbb{Z}^2} \mathbb{1}\left(\frac{\theta_{a,b,\mathbf{r}} - \theta'_{a,b,\mathbf{r}}}{\theta'_{a,b,\mathbf{r}^*}} = \frac{\theta_{0,1,\mathbf{r}} - \theta'_{0,1,\mathbf{r}}}{\theta'_{0,1,\mathbf{r}^*}}\right).$$

It is easy to see that an accepted Split move is reversed by a Merge move if the sampled relative position \mathbf{r}^* and the generated vector of weights \boldsymbol{w} is the same for both moves. This fact also produces an analytical simplification in the ratio of proposal densities, required for computing the acceptance ratio in the Metropolis-Hastings algorithm, for these moves as

$$\frac{\kappa_m(\boldsymbol{\theta}, \mathcal{R} | \boldsymbol{\theta}', \mathcal{R}')}{\kappa_s(\boldsymbol{\theta}', \mathcal{R}' | \boldsymbol{\theta}, \mathcal{R})} = \frac{|\mathcal{R}_{\max} \setminus \mathcal{R}|}{|\mathcal{R}'|} \frac{\exp\left(\frac{-(\boldsymbol{\theta}'_{\mathbf{r}^*}^\top \boldsymbol{\theta}_{\mathbf{r}^*})}{2\sigma_s^2}\right)}{(2\pi\sigma_s^2)^{d/2}}, \quad (9)$$

for any pair of states $(\mathcal{R}, \boldsymbol{\theta})$ and $(\mathcal{R}', \boldsymbol{\theta}')$ such that $\kappa_s(\boldsymbol{\theta}', \mathcal{R}' | \boldsymbol{\theta}, \mathcal{R}) > 0$. The ratio of proposal densities for the reversed transitions can be achieved by applying the inverse of (9).

Mixture proposal density. Each move described previously has a different goal in terms of how a region (in terms of both RPS and interaction coefficients) of much higher posterior density could be proposed with some probability improving the rate of convergence of the Metropolis-Hastings algorithm to a region corresponding to a global maximum. In order to assemble the five groups of moves into a single transition kernel, we define a proposal density κ that is composed by a mixture of the of five described densities

$$\kappa(\boldsymbol{\theta}', \mathcal{R}' | \boldsymbol{\theta}, \mathcal{R}) = \sum_{\Psi \in \{\text{w}, \text{bd}, \text{sw}, \text{m}, \text{s}\}} p_\Psi(\mathcal{R}) \kappa_\Psi(\boldsymbol{\theta}', \mathcal{R}' | \boldsymbol{\theta}, \mathcal{R}), \quad (10)$$

where $p_\Psi(\mathcal{R})$ corresponds to the probability of selecting a move Ψ when the current state has the RPS component as \mathcal{R} and $\sum_\Psi p_\Psi(\mathcal{R}) = 1$. Having the mixture probabilities depend on the current RPS is required to avoid undefined behaviors such as proposing a random walk move κ_w when we have an empty RPS, $\mathcal{R} = \emptyset$.

Following [Green \(1995\)](#) and [Brooks et al. \(2003\)](#), we can describe the acceptance of the Metropolis-Hastings (Reversible Jump) algorithm when using a mixture proposal density by using the ratio of the sampled move Ψ at each step,

$$\mathcal{A}_\Psi(\boldsymbol{\theta}', \mathcal{R}' | \boldsymbol{\theta}, \mathcal{R}) = \frac{q(\mathcal{R}')}{q(\mathcal{R})} \frac{\pi(\boldsymbol{\theta}' | \mathcal{R}')}{\pi(\boldsymbol{\theta} | \mathcal{R})} \frac{\tilde{f}(\boldsymbol{\theta}', \mathcal{R}')}{\tilde{f}(\boldsymbol{\theta}, \mathcal{R})} \frac{p_{\Psi'}(\mathcal{R})}{p_\Psi(\mathcal{R})} \frac{\kappa_{\Psi'}(\boldsymbol{\theta}, \mathcal{R} | \boldsymbol{\theta}', \mathcal{R}')}{\kappa_\Psi(\boldsymbol{\theta}', \mathcal{R}' | \boldsymbol{\theta}, \mathcal{R})}, \quad (11)$$

where Ψ' is the inverse move of the move Ψ , i.e., $\Psi' = \Psi$ if $\Psi = w, bd$ or sw and swapped for $\Psi = s$ or m . The complete procedure is described in [Algorithm 1](#). In practice, computations involving $\mathcal{A}_\Psi(\cdot, \cdot | \cdot, \cdot)$ can be performed in logarithmic scale for both analytical and numerical simplicity.

Algorithm 1: Metropolis-Hastings algorithm with mixture proposal density.

```

Set the initial state  $(\mathcal{R}^{(0)}, \boldsymbol{\theta}^{(0)})$ ;
foreach  $t = 0, \dots, n_{iter}$  do
    Sample a random move  $\Psi$  from  $\{w, bd, sw, s, m\}$  with probabilities
         $p_w(\mathcal{R}^{(t)}), p_{bd}(\mathcal{R}^{(t)}), p_{sw}(\mathcal{R}^{(t)}), p_s(\mathcal{R}^{(t)}), p_m(\mathcal{R}^{(t)})$ ;
    Propose a new state  $(\mathcal{R}', \boldsymbol{\theta}')$  by sampling from the proposal density
         $\kappa_\Psi(\cdot, \cdot | \mathcal{R}^{(t)}, \boldsymbol{\theta}^{(t)})$ ;
    Compute the Acceptance Ratio  $\mathcal{A}(\mathcal{R}', \boldsymbol{\theta}' | \mathcal{R}^{(t)}, \boldsymbol{\theta}^{(t)})$  from (11);
    if  $U < \mathcal{A}(\mathcal{R}', \boldsymbol{\theta}' | \mathcal{R}^{(t)}, \boldsymbol{\theta}^{(t)})$  then
        |  $(\mathcal{R}^{(t+1)}, \boldsymbol{\theta}^{(t+1)}) \leftarrow (\mathcal{R}', \boldsymbol{\theta}')$ 
    else
        |  $(\mathcal{R}^{(t+1)}, \boldsymbol{\theta}^{(t+1)}) \leftarrow (\mathcal{R}^{(t)}, \boldsymbol{\theta}^{(t)})$ 

```

3.3 Prior Distributions Specification

An important element of Bayesian Inference is the choice of prior distributions for the unobserved quantities. While these distributions are meant to reflect previous information that can be accounted in the model, the general forms of these distributions are often restricted to a specific family, that have good analytical and computational properties, while still preserving some flexibility to include prior information in the form of hyper-parameters that may have useful interpretations depending on the family of prior distributions.

In this work, for the prior distribution of the RPS, $q(\mathcal{R})$, we consider a class of probability functions proportional to a function that penalizes complex models

$$q(\mathcal{R}) = \frac{\beta^{-\alpha d|\mathcal{R}|}}{\eta_{\mathcal{M}}(\alpha, \beta)}, \quad (12)$$

where $\alpha > 0$ and $\beta > 0$ are hyper-parameters that can be interpreted as composing a multiplicative penalty introduced for each additional relative position introduced and $\eta_{\mathcal{M}}(\alpha, \beta) = \sum_{\mathcal{R}' \in \mathcal{M}} \beta^{-\alpha d|\mathcal{R}'|}$ is a normalizing constant so that q is a proper distribution on \mathcal{M} .

Note that the ratio for two RPSs, \mathcal{R} and \mathcal{R}' , $q(\mathcal{R})/q(\mathcal{R}') = \beta^{\alpha d(|\mathcal{R}'| - |\mathcal{R}|)}$, is an important quantity for the acceptance ratios of the Reversible-Jump proposal described in (11). There are key interpretations for this value such as, any two RPSs with the same number of relative positions have the same values for the function q , simplifying the expression for moves that preserve the complexity of

the RPS. Also, $q(\mathcal{R})/q(\mathcal{R}') = \beta^{-\alpha d}$ when $|\mathcal{R}| = |\mathcal{R}'| + 1$, which corresponds to all the other proposal moves that include or exclude positions one at time.

For the prior distribution of $\boldsymbol{\theta}$ given a RPS, $\phi(\boldsymbol{\theta}|\mathcal{R})$, a standard choice is to use independent normal distributions, with a given fixed prior variance, σ_p^2 , and zero mean, i.e.,

$$\phi(\boldsymbol{\theta}|\mathcal{R}) = \frac{1}{(2\pi\sigma_p^2)^{|\mathcal{R}|d/2}} \exp\left(-\frac{1}{2\sigma_p^2} \sum_{\mathbf{r} \in \mathcal{R}} \boldsymbol{\theta}_{\mathbf{r}}^\top \boldsymbol{\theta}_{\mathbf{r}}\right). \quad (13)$$

One of the main advantages of this prior distribution is that ratios, $\phi(\boldsymbol{\theta}|\mathcal{R})/\phi(\boldsymbol{\theta}'|\mathcal{R}')$, used for computing acceptance ratios of the RJMCMC algorithm described previously, can be computed more efficiently due to advantages from good analytical properties. For example, the ratio is always 1 for Position Swap moves and the density (or the inverse of) of a d -dimensional Normal distribution for Birth and Death moves. Since those computations are carried in logarithmic scale, most of the terms involving $\boldsymbol{\theta}$ will be sums of quadratic forms that are simple to evaluate.

4 Simulation Study

In order to validate the practical use of the proposed RJMCMC algorithm and understand the effect of the RPS prior distribution choice on the selected models, we conducted a simulation study where three MRFs on a 150×150 lattice, $\mathbf{Z}^{(i)}$, were simulated using sparse interaction structures $\mathcal{R}^{(i)}$, $i = 1, 2, 3$, and alphabet $\mathcal{Z} = \{0, 1, 2\}$. The sparse RPSs considered have increasing complexity and are specified as follows:

- $\mathcal{R}_1 = \{(1, 0), (0, 1)\}$,
- $\mathcal{R}_2 = \{(1, 0), (0, 1), (3, 3)\}$,
- $\mathcal{R}_3 = \{(1, 0), (0, 1), (3, 3), (3, 0)\}$,

and for the maximal RPS we considered \mathcal{R}_{\max} containing all relative positions within a maximum distance of 5 from the origin, excluding positions that are the opposite of another one included to ensure that it is a proper RPS, as illustrated in [Figure 5](#).

With $|\mathcal{Z}| = 3$, a total of $d = 8$ coefficients may vary for each relative position \mathbf{r} , therefore, \mathcal{R}_{\max} , which has a total of 60 positions, is associated with 480 free interaction coefficients when every relative position is included, whereas \mathcal{R}_3 , the most complex of the three RPSs that generated the data, represents a model with 32 free interaction coefficients. This reduction from 480 to 32 (or less) free quantities in a model may be extremely useful for inference by reducing complexity and computational cost, as long as the interactions, within the selected set of relative positions, can capture most of the dependence structure of the data.

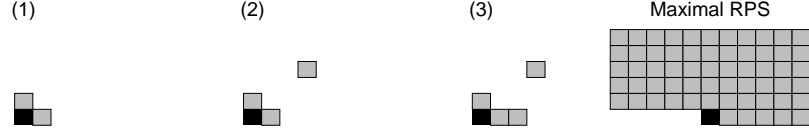


Figure 5: Interaction structures considered in simulations \mathcal{R}_i , $i = 1, 2, 3$ and maximal interaction structure \mathcal{R}_{\max} considered in the reversible jump algorithm.

We considered the same interaction coefficients $\theta_{a,b,\mathbf{r}}$ across simulations for overlapping positions \mathbf{r} with values described in Table 1 and the simulated observations are presented in Figure 6. The coefficient values were selected to generate different patterns between sampled images and it is not clear, especially for the second and third simulated fields, which set of relative position best describes the patterns generated.

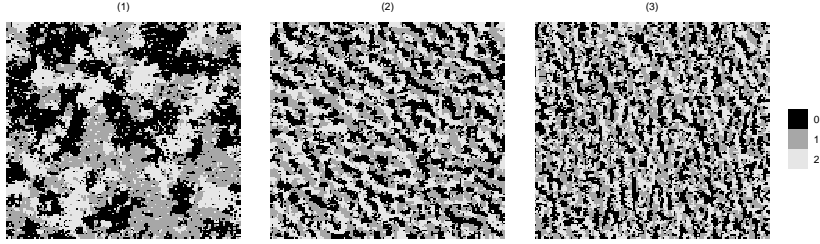


Figure 6: Simulated 150×150 MRFs $\mathbf{z}^{(i)}$, $i = 1, 2, 3$.

Table 1: $\theta_{a,b,\mathbf{r}}$ used in simulations.

\mathbf{r}	a	$b = 0$	$b = 1$	$b = 2$	\mathbf{r}	a	$b = 0$	$b = 1$	$b = 2$
(1, 0)	0		-1.0	-1.0	(1, 0)	0		-1.0	-1.0
	1	-1.0	0.0	-1.0		1	-1.0	0.0	-1.0
	2	-1.0	-1.0	0.0		2	-1.0	-1.0	0.0
(3, 3)	0		0.3	0.3	(3, 0)	0		0.3	0.3
	1	0.3	0.0	0.3		1	0.3	0.0	0.3
	2	0.3	0.3	0.0		2	0.3	0.3	0.0

Prior Distributions and Algorithm tuning. For the RPS prior distribution, we considered $q(\mathcal{R})$ as in (12), taking $\beta = |\mathcal{S}|$ and we ran the algorithm over a grid of 10 values for $\alpha \in \{0, 0.1, 0.5, 1, 1.5, 2, 2.5, 3, 5, 10\}$ for each simulation. This specific setup corresponds to a prior distribution over the RPS that can interpreted as a penalty to larger-complexity models similar to the penalty

introduced when using the Bayesian Information Criterion (BIC). When looking at the pseudoposterior in logarithmic scale, an additive term, $-\alpha d|\mathcal{R}| \log(|\mathcal{S}|)$, appears with $d|\mathcal{R}|$ being the number of free parameters of the model and $|\mathcal{S}|$ can be roughly interpreted as the sample size. The value of α controls the penalty on the prior probability for more complex models and it is directly related to how complex the higher pseudoposterior models tend to be, with a larger value of α leading to more mass concentrated on simpler models. Since the coefficients themselves are hardly interpretable, we chose to use vague priors for varying-dimensional vector $\boldsymbol{\theta}$, considering independent Gaussian priors with mean 0 variance and prior variance of $\sigma_p^2 = 10$ for each of its components, regardless of the RPS associated with it.

As for the parameters involved in the proposal kernel, we executed multiple short pilot runs to evaluate whether high pseudoposterior regions (RPS and coefficients) were reached within a sensible number of iterations and acceptance rates were at a reasonable level. We concluded that $\sigma_s^2 = \sigma_{\text{bd}}^2 = 0.15$, $\sigma_w^2 = 0.005$ and $\nu = 0.1$ resulted in good balance between exploring the complex space that is composed by the RPS and the varying-dimension coefficient vector while maintaining the acceptance rate at reasonable levels. Low values for ν should be used in order to “concentrate” the weights sampled from the Dirichlet distribution in a few values when proposing a Split move.

For the mixture probabilities probabilities, we chose $p_\Psi(\mathcal{R})$ always proportional to 4 for $\Psi = w$ and 1 for the remaining types of moves that are valid for the current state \mathcal{R} , resulting in

$$\begin{aligned} p_w(\mathcal{R}) &\propto 4\mathbb{1}(\mathcal{R} \neq \emptyset), & p_{\text{bd}}(\mathcal{R}) &\propto 1, \\ p_{\text{sw}}(\mathcal{R}) &\propto \mathbb{1}(\mathcal{R} \neq \mathcal{R}_{\text{max}}, \mathcal{R} \neq \emptyset), \\ p_{\text{m}}(\mathcal{R}) &\propto \mathbb{1}(\mathcal{R} \neq \mathcal{R}_{\text{max}}, \mathcal{R} \neq \emptyset), & p_{\text{d}}(\mathcal{R}) &\propto \mathbb{1}(\mathcal{R} \neq \mathcal{R}_{\text{max}}, \mathcal{R} \neq \emptyset). \end{aligned} \tag{14}$$

It is important to note that not every type of move is well-defined and not constant for every RPS. For example, a random walk move cannot propose anything meaningful when $\mathcal{R} = \emptyset$, regardless of how it is defined, and a swap move cannot be completed with $\mathcal{R} = \mathcal{R}_{\text{max}}$. This “prohibitions” introduced by setting some probabilities to zero ensure that we never propose moves that result in the exact same values of the current state, which would add no meaningful information to the sampled chain while demanding computing resources.

The **initial state** of the chain is another factor that should be controlled in order reach equilibrium with less iterations. Since the proposal distribution was designed mainly to propose new points that jump between the modes of the coefficient distributions for different RPSs that follow certain properties, better mixing is achieved when the initial state has coefficients near the mode of the pseudoposterior for the initial RPS. In order to obtain a reasonable initial state, we chose to use a warm-up run of 5000 iterations starting with \mathcal{R}_{max} and only proposing points using the random walk move, i.e., $p_w(\mathcal{R}_{\text{max}}) = 1$ in the warm-up run. This results in a chain that slowly drifts towards the region of the mode of coefficient values associated with \mathcal{R}_{max} . We used the last sampled state of this warm-up run as the initial state for the actual Reversible Jump

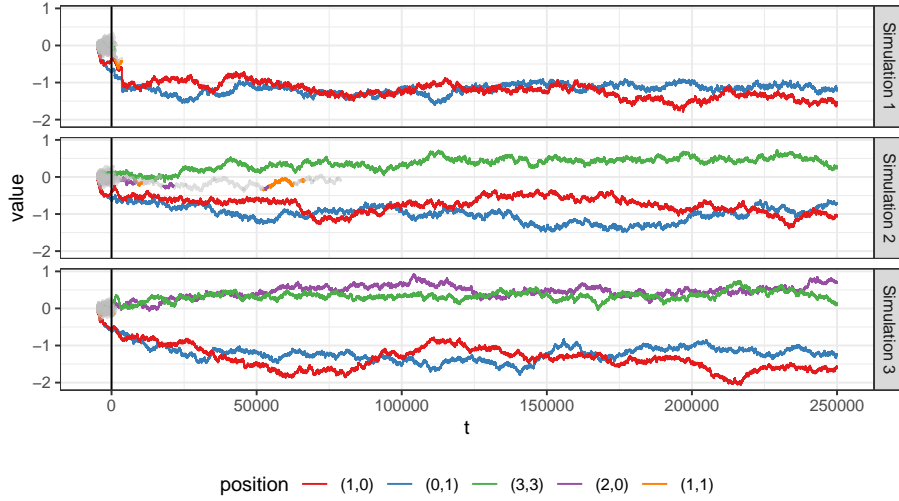


Figure 7: Values of the RJMCMC sampled for the interaction coefficients $\theta_{\mathbf{r},1,0}$ for multiple relative positions \mathbf{r} in each simulation with $\alpha = 1.5$. Coefficients associated with some particular set of relative positions are highlighted and colored and the remaining ones are represented with gray lines. Iterations of the warm-up run are indexed -4999 to 0.

run.

Results. In all thirty simulations (3 models \times 10 α -values), the Markov chain sampled in the warm-up stage quickly converged to a stable distribution suggesting that the initial state used for the RJMCMC was close to a sample taken from the coefficients pseudoposterior for the maximal RPS.

Figure 7 illustrates the sampled chain behavior in each simulation for a specific value of α and each interaction coefficient. Coefficients associated with some relevant positions are highlighted and colored so they can be tracked across iterations. The values for iterations in the warm-up stage (indexed by $t < 0$) cannot be clearly identified as the coefficients for all 60 positions are included in this stage, but as the main Reversible Jump run starts, the number of positions included quickly reduces to no more than 4 within a few iterations. In this figure, lines may “appear” or “disappear” as relative positions are included or excluded, respectively, from the sampled RPS, and lines may change colors when swap moves are accepted.

For every chain sampled with more strict RPS priors ($\alpha \geq 1$), after moves between different RPSs, the Reversible Jump algorithm reached a state where only moves within the same RPS (random walk moves) were accepted, even when different relative positions were being constantly proposed. This “final” RPS varies depending on the simulation (as in the examples of Figure 7) and

the value of α . As α increases, the chains converge to smaller RPSs excluding some positions that were part of the RPS used for simulating the data. Under less penalizing priors ($\alpha \leq 1$), supersets of the RPS used in the simulation were obtained in the chains, with the exceeding relative positions constantly switching.

While visualizing sets of relative positions or the multiple coefficients with varying dimensions involved is not possible, we can use the marginal proportions which each relative position appears in the sampled chain as a quick way to understand which positions are more relevant for that run. Figures 8, 9 and 10 present these proportions for all the values of α used in simulations 1, 2 and 3, respectively. These proportions were computed with a burn-in of 100000 iterations and sampling only multiples of 10 to reduce serial correlation, so that we can conclude that a run mostly concentrated in a few relative positions not only had those positions included in most of the iterations, but also converged to that final RPS quickly removing unnecessary positions in the burn-in period.

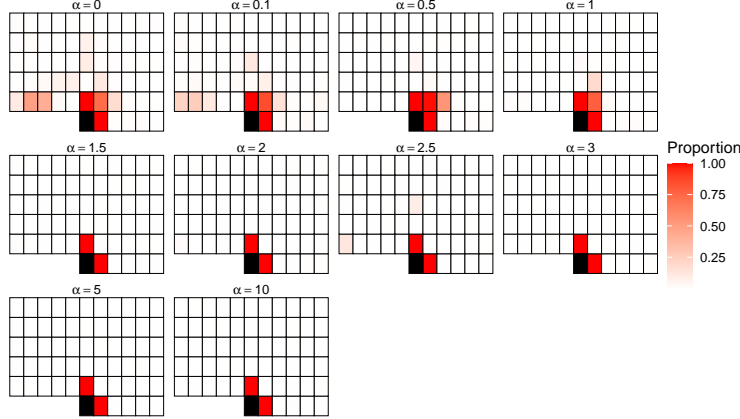


Figure 8: Marginal pseudoposterior probabilities estimated of the inclusion of each relative position for Simulation 1, varying the prior distribution of the RPS, $q(\mathcal{R})$, according to α .

Considering the results obtained, we conclude that for the simulated scenarios, a prior distribution with $\alpha = 1.5$ or 2 converges rapidly and leads to consistent results concentrating high pseudoposterior mass on the RPS that was used to generate the data. In fact, in the proposed study, the algorithm was successful in identifying the RPS that generated the data when applying the sparse estimator from (6) for many levels of thresholding constants especially for $\alpha = 1.5$ and 2. It is an interesting fact that $\alpha = 2$ makes the prior distribution numerically equivalent to the penalty used by the Bayesian Information Criterion (BIC) used for model (variable) selection.

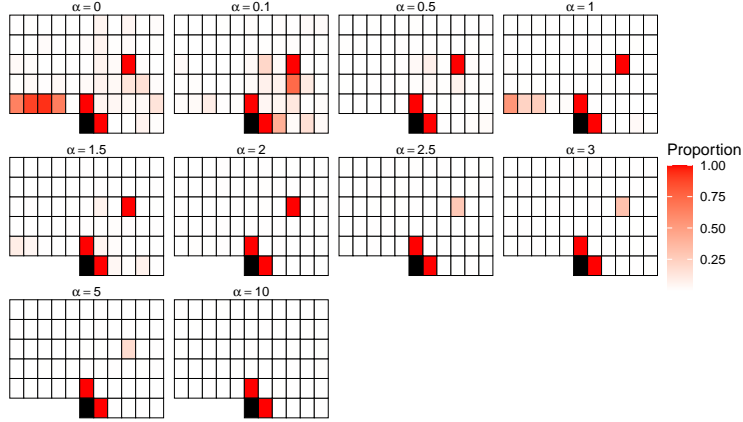


Figure 9: Marginal pseudoposterior probabilities estimated of the inclusion of each relative position for Simulation 3, varying the prior distribution of the RPS, $q(\mathcal{R})$, according to α .

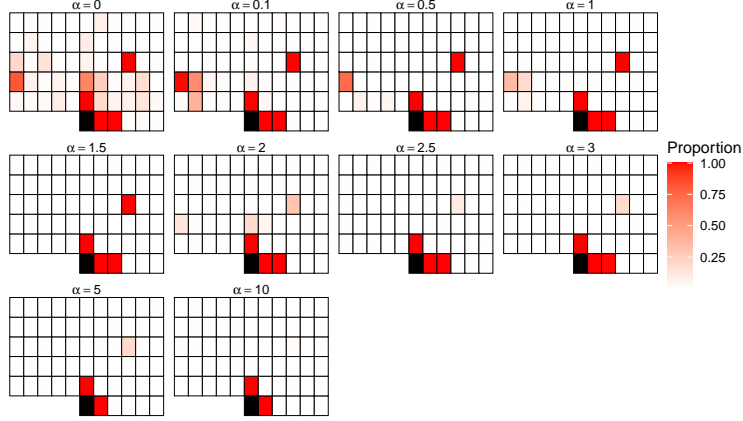


Figure 10: Marginal pseudoposterior probabilities estimated of the inclusion of each relative position for Simulation 3, varying the prior distribution of the RPS, $q(\mathcal{R})$, according to α .

5 Application to Synthesis of Texture Image

In order to evaluate the proposed model selection methodology in a real data context, we apply the proposed algorithm to a discrete texture image obtained as a result of the textile images analysis in [Freguglia et al. \(2020\)](#). In the original work, a Gaussian mixture with 5 components, driven by the Markov Random Field model described in [Section 2](#), is used to describe grayscale continuous-valued images of dyed textiles and one of the products of the analysis is a pixel-wise segmentation of which mixture component was estimated as the most

probable. The interaction coefficients of the hidden MRF were originally estimated considering a complete region, with every position within a maximum distance of 5, but we are interested in investigating whether similar interactions for the mixtures components could be described by sparser interaction structures, producing synthetic texture images that have the same patterns as the reference image. We will consider the 200 by 200 subset of one of the estimated discrete images presented in [Figure 11](#), and denote it as \mathbf{z}^* .

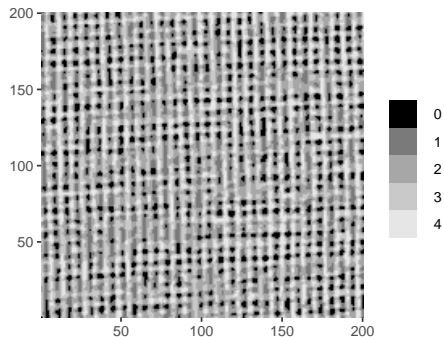


Figure 11: A 200 by 200 pixels texture image with 5 colors ($C = 4$), denoted \mathbf{z}^* .

Considering as input the image data from [Figure 11](#), our goal is to determine whether the complete interaction structure is necessary to properly model the observed random field or a sparser interaction structure could be used, without significant differences in terms of statistical inference.

The search for sparse neighborhoods for modeling texture has been the subject of several papers in the literature, among them, [Cross and Jain \(1983\)](#) and [Gimel'farb \(1996\)](#). However, the selection methods used are mostly heuristic. In this work, we propose a novel statistical methodology that allows to perform proper statistical inference.

To run the algorithm, we consider the maximal interaction structure of the algorithm, \mathcal{R}_{\max} , as the neighborhood used in the original paper, which includes positions with maximum norm up to 5. Hyper-parameters of prior distributions and of the Reversible Jump algorithm were selected with the same values of the simulation study from [Section 4](#) and we fix the RPS prior distribution hyper-parameter α as 0.25. While values of α in this range lead to most of the pseudo-posterior mass being concentrated on a superset of the RPS used to simulated the datasets, there was still a significant reduction in the number of positions included. In practice, our goal is to keep all the positions required to probabilistically describe the texture pattern while controlling the number of free coefficients by selecting a RPS that is sparse when compared to the complete region originally used.

We ran 500,000 iterations of the proposed Reversible-Jump algorithm after 10,000 warm-up iterations where the random walk move was selected with

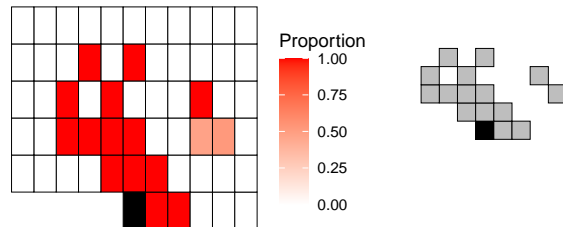


Figure 12: Map with the proportions of times each relative position is included in the RPS sampled within final (left) and the sparse interaction structure selected with a 0.5 thresholding value $\hat{\mathcal{R}}_{\text{sp}}(0.5)$ (right).

probability 1, starting from the maximal RPS. In the same way as described for the simulation study from [Section 4](#), we stated the RJMCMC in an initial state close to a sample of the pseudoposterior for the maximal \mathcal{R}_{max} . The proportions each relative position in \mathcal{R}_{max} appear in the sampled chain are presented in [Figure 12](#). Given the pseudoposterior distribution, we used the thresholding RPS estimator strategy from [\(6\)](#) with a value of $c_{\text{th}} = 0.5$ to select one sparse interaction structure to be used in our result analysis, with a reduction from 60 to 15 relative positions, which corresponds to a reduction of $45 \times 24 = 1125$ free coefficients in the model. Other results could be drawn from RPS pseudoposterior distribution for model selection purposes, such as the set of highest pseudoposterior RPSs or the pseudoposterior probability of a group of RPSs with specific characteristics, depending on the interests of the analysis being made.

Evaluating the results. Differently from the analysis made for the simulation study presented in [Section 4](#), we do not have the interaction structure that generated the data available to compare to the RPS pseudoposterior distribution obtained. Goodness of fit evaluation strategies in a Bayesian context are proposed in [Gelman et al. \(1996\)](#) and [Bayarri and Berger \(2000\)](#), where metrics can be derived by generating realizations of the model by sampling from the posterior distribution and comparing key statistics from the reference dataset \mathbf{z}^* and those realizations. These methods are not directly applicable in our context because we only have the pseudoposterior distribution available, rather the true posterior distribution (although the differences between these two distributions could be mitigated by using methods as the pseudoposterior adjustment from [Bouranis et al. \(2017\)](#)). Moreover, we cannot define a small number of key statistic to use for the tests, as MRF texture images have a high-dimensional vector of pairwise counts as sufficient statistics.

As an alternative approach to evaluate a single sparse model that was obtained analysing the pseudoposterior distribution, we ran maximum likelihood estimation via stochastic approximation, a standard inference method used in the context of MRFs, and compared results of such inference using the selected

sparse interaction structure against the same analyses in scenarios where such sparse RPS is not available. Applying the maximum likelihood estimation via stochastic approximation, we obtain the estimated coefficients, then we generate realizations of the MRF using the estimated coefficients and compare useful statistics for describing the texture from the generated samples and the target dataset \mathbf{z}^* .

We considered 3 different reference RPSs for comparison:

1. $\mathcal{R}_{\text{nn}} = \{(1, 0), (0, 1)\}$: A nearest-neighbor RPS that we will use as a benchmark in comparisons.
2. \mathcal{R}_{sp} : The sparse RPS obtained using the thresholding estimator for our specific thresholding constant choice presented in [Figure 12](#).
3. \mathcal{R}_{max} : The maximal set of relative positions, containing all relative positions within maximum distance of 5, as used in the original paper.

and our goal is to evaluate whether completing an analysis using \mathcal{R}_{sp} leads to results at least as accurate as obtained using \mathcal{R}_{max} , and at the same time understand how relevant the differences were when compared to the estimates obtained when using a naive model choice with \mathcal{R}_{nn} .

We used the Stochastic Approximation algorithm ([Robbins and Monro, 1951](#)) to obtain a Maximum Likelihood estimate of the coefficients for each of the three described RPSs. The algorithm consists of iteratively updating the solution according to a step size sequence $\gamma_{t \geq 0}^t$ and an estimate of the gradient function, that depends on the sufficient statistic of the model, $T(\cdot)$, computed on the reference dataset \mathbf{z}^* and on a realization, $\mathbf{z}^{(t)}$, of the random field simulated from the current coefficients (see [Freguglia and Garcia \(2022\)](#) for more details on the Stochastic Approximation algorithm used). The algorithm is described by the recursion

$$\boldsymbol{\theta}^{(t+1)} = \boldsymbol{\theta}^{(t)} + \gamma^{(t)} \left(T(\mathbf{z}^*) - T(\mathbf{z}^{(t)}) \right), \quad (15)$$

with $\gamma^{(t)}$ being a decreasing sequence. Note that the sufficient statistics $T(\cdot)$ has the same dimension as the vector of free coefficients $\boldsymbol{\theta}$ and, therefore, its indexing and dimension also depends on the associated RPS. We used the proper definitions of $T(\cdot)$ for each of the three RPSs used.

We ran 1500 steps of (15) with $\gamma^{(t)} = \frac{1500-t}{1500}$ starting from the zero-valued coefficient vector $\boldsymbol{\theta}_{a,b,\mathbf{r}} = 0$ for every a, b, \mathbf{r} for each of the three RPSs to obtain maximum likelihood estimates of coefficients in each case. Then, we generated 100 samples from each of three models with the estimated coefficients, which we will denote $\tilde{\mathbf{z}}_{\text{nn}} = \left(\mathbf{z}_{\text{nn}}^{(v)} \right)$, $\tilde{\mathbf{z}}_{\text{sp}} = \left(\mathbf{z}_{\text{sp}}^{(v)} \right)$ and $\tilde{\mathbf{z}}_{\text{max}} = \left(\mathbf{z}_{\text{max}}^{(v)} \right)$, $v = 1, \dots, 100$, for \mathcal{R}_{nn} , \mathcal{R}_{sp} and \mathcal{R}_{max} respectively, (the tilde symbol is used to stress the fact that it is a set of MRF realizations). Examples of one of the simulated images for each of the three scenarios considered are presented in [Figure 13](#). Notice that the first image generated from the Nearest-Neighbor model completely misses

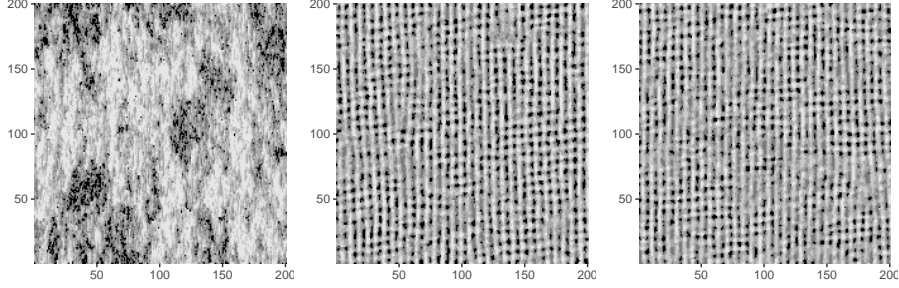


Figure 13: Simulated realizations of the MRF model obtained from the Maximum Likelihood estimate considering a Nearest-Neighborhood structure (left), Estimated Sparse interaction structure (middle) and Maximal interaction structure (right).

the features of the texture, whereas there is not much difference between the one generated with the sparse model and the full one.

Finally, we define $\rho_{a,b,\mathbf{r}}(\mathbf{z}) = \sum_{\mathbf{i} \in S} \mathbb{1}(z_{\mathbf{i}} = a, z_{\mathbf{i}+\mathbf{r}} = b)$ as the count of occurrences of the pair (a, b) within relative position \mathbf{r} (this is part of the vector of sufficient statistics of the model when \mathbf{r} is included in the RPS). To summarize this information, we compute the average counts for a set of realizations as

$$\bar{\rho}_{a,b,\mathbf{r}}(\tilde{\mathbf{z}}) = \sum_{v=1}^{100} \frac{\rho_{a,b,\mathbf{r}}(\mathbf{z}^{(v)})}{100},$$

and the metric

$$\Delta(\tilde{\mathbf{z}}, \mathbf{z}^*) = \log \left(\sqrt{\sum_{a \in \mathcal{Z}} \sum_{b \in \mathcal{Z}} \sum_{\mathbf{r} \in \mathcal{R}_{\max}} (\rho_{a,b,\mathbf{r}}(\mathbf{z}^*) - \bar{\rho}_{a,b,\mathbf{r}}(\tilde{\mathbf{z}}))^2} \right),$$

which represents the logarithm of the Euclidean distance between the vector containing all the pairwise counts for relative positions in the maximal RPS and the average vector of pairwise counts in the set of samples $\tilde{\mathbf{z}}$ for the same relative positions. This is a measure of similarity between the patterns generated from each model and the observed sample \mathbf{z}^* . The smaller the value of $\Delta(\tilde{\mathbf{z}}, \mathbf{z}^*)$, the closer the pairwise counts of the reference field \mathbf{z}^* to their expected values are (approximated by the samples average) under a model with that specific RPS and its associated maximum likelihood estimators for the coefficients. Note that we have used the counts in every relative position of the maximal RPS, \mathcal{R}_{\max} , because we want to ensure not only the counts of relative positions included in the RPS used for estimation are similar to \mathbf{z}^* , but also for a larger common set of statistics across the three scenarios.

As pointed before, looking at the generated samples displayed in [Figure 13](#), the image generated from \mathcal{R}_{nn} have a completely different pattern than the original dataset \mathbf{z}^* and both the examples generated \mathcal{R}_{sp} and \mathcal{R}_{max} presented

Table 2: $\Delta(\tilde{\mathbf{z}}, \mathbf{z}^*)$ values considering the three sets of samples generated from the model estimated with different RPSs.

RPS	\mathcal{R}_{nn}	\mathcal{R}_{sp}	\mathcal{R}_{max}
$\Delta(\tilde{\mathbf{z}}, \mathbf{z}^*)$	10.6092	8.1320	9.5734

patterns very similar when compared to \mathbf{z}^* . This is confirmed comparing the values of the computed values $\Delta(\tilde{\mathbf{z}}, \mathbf{z}^*)$ presented in Table 2. We see that, as expected, the model estimated using the benchmark nearest-neighbor structure presented the highest distance between pairwise counts of \mathbf{z}^* and their expected values in the model, and the model estimated from \mathcal{R}_{sp} had their expected statistics closer to the observed in \mathbf{z}^* than the ones computed using \mathcal{R}_{max} .

Therefore, we conclude that estimating coefficients from a sparse interaction structure, obtained by thresholding the marginal RPS pseudoposterior distribution obtained from our proposed algorithm, has lead to improved maximum likelihood estimation, both in terms of computational costs, since there was significantly less coefficients to compute, and in terms of how similar the expected value of wide set of statistics is from the observed field used for estimation.

6 Conclusion

We propose a novel approach to model selection in Markov Random Field models with pairwise interactions in a Bayesian context by using a Reversible Jump Markov Chain algorithm with a proposal distribution that was developed especially aiming for efficient jumping between sets of relative positions, quickly reaching the models with highest posterior mass.

In order to overcome the intractability of the normalizing constant inherent from MRF models, we have used pseudolikelihood and proceeded with the analyses based on the pseudoposterior distribution as a proxy of the true posterior distribution that cannot be evaluated directly. It must be clear that the algorithm proposed can be directly adapted for different strategies that may be used to deal with the intractable constants and approximate likelihood function, such as Adjusted Pseudolikelihoods (Bouranis et al., 2018a) and Monte-Carlo approximations (Atchadé et al., 2013), but not every approximation method is well suited for the varying-dimension feature of the model selection framework.

The main contributions of this work are:

1. Proposing a Bayesian framework for both the interaction structure and the parameters of the Markov Random Field model considered.
2. Constructing a Reversible Jump proposal kernel that is especially useful for models within the proposed framework.
3. Exploring the effects of the prior distribution specification in some scenarios to understand their properties while still attaining enough flexibility in the methods so that any choice of prior distribution can be considered.

We have used artificially generated datasets and an application to real data in the context of texture synthesis, to evaluate the strengths of our method and study how the algorithm behaves under different configurations and concluded that our method leads to promising results for selecting sparse interaction structures for MRFs.

New methods for approximating the likelihood function (and the posterior distribution as a consequence) that can produce good approximations across the varying-dimension spaces, as an alternative to the pseudolikelihood would be an improvement on the proposed method. However, the biggest challenge to be addressed in a future work is the development of a constant free procedure for model selection that does not need the specification ad hoc of the penalty constant α .

The reproducible R language code is available as part of the R package **mrf2dbayes**, available in <https://github.com/Freguglia/mrf2dbayes>. It leverages the data structures provided by the **mrf2d** package (Freguglia and Garcia, 2022) and extends it by introducing additional Bayesian analysis elements such as the likelihood approximation method (in this work, the pseudolikelihood) and Metropolis-Hastings algorithms. The source code used to reproduce the results in this work is available upon request.

Acknowledgments

This work was funded by Fundação de Amparo à Pesquisa do Estado de São Paulo - FAPESP grants 2017/25469-2, 2017/10555-0, CNPq grant 304148/2020-2, and by Coordenação de Aperfeiçoamento de Pessoal de Nível Superior - Brasil (CAPES) - Finance Code 001.

References

- Arnesen, P. and Tjelmeland, H. (2017). Prior specification of neighbourhood and interaction structure in binary markov random fields. *Statistics and Computing*, 27(3):737–756.
- Atchadé, Y. F., Lartillot, N., and Robert, C. (2013). Bayesian computation for statistical models with intractable normalizing constants. *Brazilian Journal of Probability and Statistics*, 27(4):416–436.
- Bayarri, M. and Berger, J. O. (2000). P values for composite null models. *Journal of the American Statistical Association*, 95(452):1127–1142.
- Besag, J. (1975). Statistical analysis of non-lattice data. *Journal of the Royal Statistical Society: Series D (The Statistician)*, 24(3):179–195.
- Blake, A., Kohli, P., and Rother, C. (2011). *Markov random fields for vision and image processing*. MIT press.

- Boland, A., Friel, N., and Maire, F. (2018). Efficient mcmc for gibbs random fields using pre-computation. *Electronic Journal of Statistics*, 12(2):4138–4179.
- Bouranis, L., Friel, N., and Maire, F. (2017). Efficient bayesian inference for exponential random graph models by correcting the pseudo-posterior distribution. *Social Networks*, 50:98–108.
- Bouranis, L., Friel, N., and Maire, F. (2018a). Bayesian model selection for exponential random graph models via adjusted pseudolikelihoods. *Journal of Computational and Graphical Statistics*, 27(3):516–528.
- Bouranis, L., Friel, N., and Maire, F. (2018b). Model comparison for gibbs random fields using noisy reversible jump markov chain monte carlo. *Computational Statistics & Data Analysis*, 128:221–241.
- Brooks, S. P., Giudici, P., and Roberts, G. O. (2003). Efficient construction of reversible jump markov chain monte carlo proposal distributions. *Journal of the Royal Statistical Society: Series B (Statistical Methodology)*, 65(1):3–39.
- Caimo, A. and Mira, A. (2015). Efficient computational strategies for doubly intractable problems with applications to bayesian social networks. *Statistics and Computing*, 25(1):113–125.
- Cross, G. R. and Jain, A. K. (1983). Markov random field texture models. *IEEE Transactions on Pattern Analysis and Machine Intelligence*, (1):25–39.
- Csiszár, I. and Talata, Z. (2006). Consistent estimation of the basic neighborhood of markov random fields. *The Annals of Statistics*, 34(1):123–145.
- Freguglia, V. and Garcia, N. L. (2022). Inference tools for Markov random fields on lattices: The R package mrf2d. *Journal of Statistical Software*, 101(8):1–36.
- Freguglia, V., Garcia, N. L., and Bicas, J. L. (2020). Hidden markov random field models applied to color homogeneity evaluation in dyed textile images. *Environmetrics*, 31(4):e2613.
- Gelman, A., Meng, X.-L., and Stern, H. (1996). Posterior predictive assessment of model fitness via realized discrepancies. *Statistica sinica*, pages 733–760.
- Gimel'farb, G. L. (1996). Texture modeling by multiple pairwise pixel interactions. *IEEE Transactions on pattern analysis and machine intelligence*, 18(11):1110–1114.
- Green, P. J. (1995). Reversible jump markov chain monte carlo computation and bayesian model determination. *Biometrika*, 82(4):711–732.
- Hassner, M. and Sklansky, J. (1981). The use of markov random fields as models of texture. In *Image Modeling*, pages 185–198. Elsevier.

- Held, K., Kops, E. R., Krause, B. J., Wells, W. M., Kikinis, R., and Muller-Gartner, H.-W. (1997). Markov random field segmentation of brain mr images. *IEEE transactions on medical imaging*, 16(6):878–886.
- Ji, C. and Seymour, L. (1996). A consistent model selection procedure for markov random fields based on penalized pseudolikelihood. *The annals of applied probability*, 6(2):423–443.
- Kato, Z., Zerubia, J., et al. (2012). Markov random fields in image segmentation. *Foundations and Trends® in Signal Processing*, 5(1–2):1–155.
- Lee, J. D. and Hastie, T. J. (2013). Structure learning of mixed graphical models. *Journal of Machine Learning Research*, 31:388–396.
- Murray, I., Ghahramani, Z., and MacKay, D. (2012). Mcmc for doubly-intractable distributions. *arXiv preprint arXiv:1206.6848*.
- Pensar, J., Nyman, H., Niiranen, J., and Corander, J. (2017). Marginal pseudo-likelihood learning of discrete markov network structures. *Bayesian analysis*, 12(4):1195–1215.
- Robbins, H. and Monro, S. (1951). A stochastic approximation method. *The annals of mathematical statistics*, pages 400–407.
- Roy, A. and Dunson, D. B. (2020). Nonparametric graphical model for counts. *Journal of Machine Learning Research*, 21(229):1–21.
- Su, C. and Borsuk, M. E. (2016). Improving structure mcmc for bayesian networks through markov blanket resampling. *The Journal of Machine Learning Research*, 17(1):4042–4061.
- Zhang, Y., Brady, M., and Smith, S. (2001). Segmentation of brain MR images through a hidden markov random field model and the expectation-maximization algorithm. *IEEE transactions on medical imaging*, 20(1):45–57.